Molecular scale deformation in the yielding behaviour of glassy polymers

J. M. Lefebvre, B. Escaig, G. Coulon and C. Picot*
Structures et Propriétés de l'Etat Solide–U.S.T. Lille, France
(Received 27 March 1985)

The compressive deformation behaviour of amorphous glassy polymers is characterized by means of small-angle neutron scattering investigation of shear bands produced under various temperature and strain-rate conditions. The resulting molecular deformation pattern is compared to macroscopic observations on the shear-banded samples.

(Keywords: glassy polymers; shear bands; small-angle neutron scattering)

INTRODUCTION

Deformation processes responsible for yielding in amorphous glassy polymers are strongly heterogeneous, i.e. a small fraction of the sample volume is concerned with the growth and propagation of 'defects' in the molecular arrangement, either in the form of more or less well-defined shear bands or as localized crazes. We restrict our approach of the non-elastic deformation of glassy polymers to the shear-banding phenomenon.

We previously described the stress-aided thermally activated growth of shear nuclei within the frame of a thermodynamic and kinetic analysis of plasticity[1,2].

Atactic polystyrene (PS) and poly(methylmethacrylate) (PMMA) samples have been compression tested at constant strain-rate for various temperature and strain-rate conditions. The results indicate the existence of two distinct yielding behaviours[3,4]:

(i) A low temperature–high strain-rate glide mode with a stress dependent free energy of activation, phenomenologically analogous to dislocation glide in crystal plasticity.

(ii) A high temperature–low strain-rate mode related to the onset of local mobilities which soften the intrinsic molecular friction of the glide process, much akin to the diffusion induced dislocation climb mechanism in crystals.

The strain-rate dependent transition temperature [5] T_c between the two modes is linked to secondary relaxation mobilities; a detailed analysis of this particular point is given elsewhere[6].

In spite of the lack of direct observation of the defective molecular arrangement in the shear bands, small-angle neutron scattering (SANS) investigations can yield a precise picture of deformed molecular coils at various correlation distances.

In a previous paper[7] we interpreted the SANS pattern of PS shear bands in terms of a geometrical model for simple shear deformation. It was shown that coil anisotropy resulted from glide mode deformation whereas the diffusional mode SANS spectra exhibited isotropic behaviour. In the latter case the question was then posed as to whether active diffusion processes might allow coils intercalations to account for the imposed deformation without altering the overall segmental distribution.

We report here on complementary SANS measurements obtained for both PS and PMMA and the results are compared with a macroscopic characterization of the deformed samples.

Sample preparation and deformation

The mixing of fully deuterated and hydrogenated species is carried out in solution using either chloroform or dioxane as a solvent at a polymer concentration of 2% by weight; the polymer is reprecipitated from the chloroform solution in methanol and carefully dried whereas the freeze-drying technique has been adopted in the case of the dioxane solution. The latter technique has been mostly used for its better convenience.

Vacuum compression moulding and notched samples machining were described previously. We would simply recall here that this is the only suitable way for producing localized shear yielding deformation at temperatures below 0.8 T_g (where the glass transition temperature is expressed in Kelvin).

During the compression test, a macroscopic shear band develops from the notch throughout the specimen; for the clarity of forthcoming discussion *Figure 1a* gives a schematic picture of sample geometry and directions of interest with respect to the SANS experiment. A one millimetre thick band is cut parallel to the $(\hat{x}_1, \hat{x}_2)$ plane in the deformed zone and the incident neutron beam comes along $\hat{x}_3$.

Corresponding typical stress–strain curves are shown in *Figure 1b* in the case of PS deformed at 287 K for two strain-rates $\dot{\varepsilon}_1 = 4.2 \times 10^{-6}\ s^{-1}$ and $\dot{\varepsilon}_2 = 1.75 \times 10^{-3}\ s^{-1}$. The band starts to propagate from the notch when the stress reaches its maximum value and it develops to the opposite surface during the stress drop. The stress plateau relates to the thickening of the deformation zone and all samples are given the same non-elastic deformation $\varepsilon_p = 0.10$, as measured from the yield point.

The internal structure of such macroscopic bands has been investigated by several authors[8–10] who find a gradual transition from slip bands to diffuse shear zones as the strain-rate is decreased. Moreover electron microscopy observations reveal that the diffuse zones also consist in fine slip bands packets[10].

In the present situation a simple macroscopic character-

Centre de Recherches sur les Macromolécules, Strasbourg, France.

0032-3861/85/121807-07$03.00

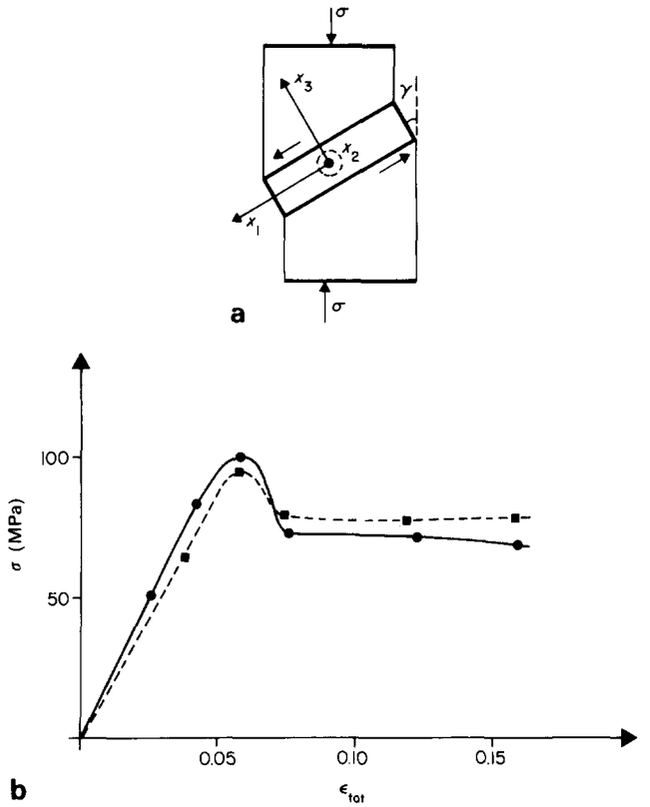

Figure 1 (a) Schematic representation of sample with reference axis. (b) Typical stress–strain curves for both glide and diffusional modes: (———) $\dot{\epsilon}_p = 1.75 \times 10^{-3}\ s^{-1}$; (-----) $= 4.2 \times 10^{-6}\ s^{-1}$

ization of the deformation has been carried out in the following way: a deformed sample is split longitudinally in two halves along the $(\hat{x}_1, \hat{x}_3)$ plane and the cut surfaces are carefully polished with aluminium paste. A scratch parallel to the former cylindrical sample axis is then drawn with a razor blade. The split specimens are heated above the glass transition temperature and they regain original shape. Measurements of post-recovery length indicate a nearly complete strain recoverability (>98%) whatever the deformation regime was.

Figures 2a and *b* show the scratch displacement induced by the reverse motion of the band for the diffusional mode (*Figure 2a*: $\dot{\epsilon}_1 = 4.2 \times 10^{-6}\ s^{-1}$) and the glide mode (*Figure 2b*: $\dot{\epsilon}_2 = 1.75 \times 10^{-3}\ s^{-1}$) situations in the case of PS at 287 K.

The surface under observation is slightly distorted after the recovery annealing; this is an indication that the average simple shear direction may not be strictly restricted to the $\hat{x}_1$ direction, i.e. an $\hat{x}_2$ component has to be taken into account as we previously reported. In fact even if this transverse contribution is very small in the present cases, it results in some difficulty to resolve the sheared zone boundaries in the optical microscope. Nevertheless as illustrated in *Figure 2a* fairly precise determination of the total strain can still be obtained.

This total shear strain is the ratio of the marker line displacement d to the thickness of the band[8] t.

On the average, we see the following results:

diffusional mode:	$0.65 < tg\gamma < 0.80$
glide-mode:	$1.15 < tg\gamma < 1.30$

where γ is the shearing angle and $tg\gamma = d/t$.

Another important parameter is the degree of strain localization in the shear band (we refer to the macroscopically sheared zone, and not to individual true shear bands). Resolving the compressive deformation into the band shows that it retains 65 to 75% of the total strain in the diffusional mode and up to 95% in the glide mode in the case of PS. The situation becomes more critical in the case of PMMA where only 55 to 60% of the total strain is confined to the band at room temperature whereas fracture occurs at the notch tip prior to shear banding when attempts have been made to deform at low temperature and moderate strain-rate to investigate the glide-mode behaviour.

Simple shear deformation and the SANS experiment

As recalled earlier, the deformation band is parallel to the $(\hat{x}_1\hat{x}_2)$ plane and shear occurs along $\hat{x}_1$ direction. The plane strain mode thus encountered implies that a sphere of matter within the band will turn into an ellipsoid without any modification of its overall dimension as viewed along $\hat{x}_2$. The band extracted from the deformed sample is submitted to the SANS experiment with the neutron beam along $\hat{x}_3$. This means that no information is available within the thickness of the band. Considering a polymer coil after deformation we thus have an indication of its elongation in the $\hat{x}_1$ direction but no check of its flattening in the $\hat{x}_3$ direction.

Nevertheless if we call R_0 the root mean square radius of gyration of the molecule in the bulk isotropic state and $R_\parallel$ and $R_\perp$ the apparent radii along $\hat{x}_1$ and $\hat{x}_2$ respectively, we have shown that the simple shear deformation yields[7]:

$$R_\perp = R_0 \qquad \text{and} \quad \frac{R_\parallel}{R_\perp} = \sqrt{1 + tg^2\gamma}$$

$$R_\parallel > R_\perp$$

where γ is the angle of shear.

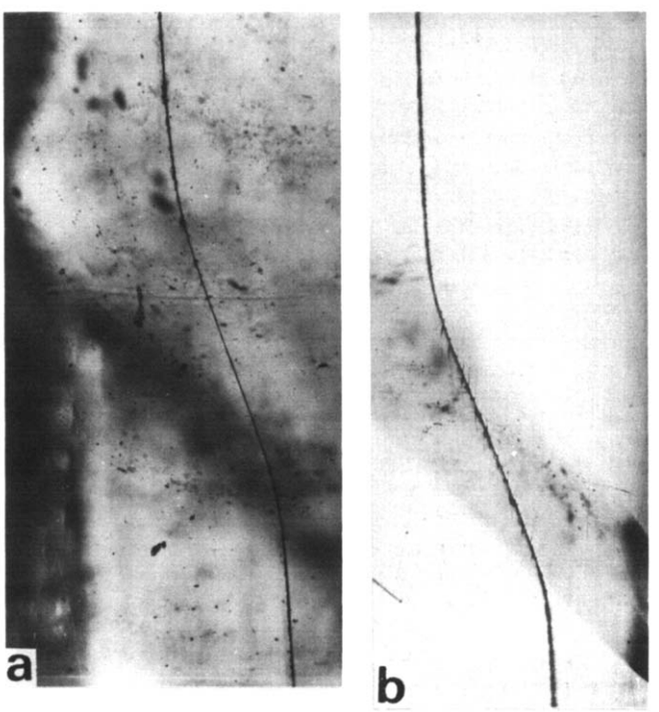

Figure 2 Characterization of strain in the macroscopic shear band—(a): diffusional mode; (b) glide mode

As for the results reported previously, the temperature and strain-rate conditions are chosen on the basis of the thermodynamic and kinetic analysis of deformation in order to investigate samples representative of either of the two modes.

In particular, for a strain-rate $\dot{\varepsilon}_p \sim 2 \times 10^{-4}\ s^{-1}$ we have the following indications[2,5]:

PMMA	$T_c \sim 245$ K
PS	$T_c \sim 290$ K

and the transition temperature T_c between the two modes is shifted upward by ~ 15 K per decade increase of the strain-rate.

The selected conditions are gathered in *Table 1* together with the samples' molecular weight characteristics.

Small-angle neutron scattering experiments

The SANS experiments were performed on the two small-angle spectrometers D_{11} and D_{17} at the Institut Laüe-Langevin (ILL), Grenoble, France. Scattering vectors $q = (4\pi/\lambda)\sin(\theta/2)$ (where θ is the scattering angle and λ is the wavelength associated to the neutron beam) lie in the range:

$$5 \times 10^{-3} < q < 2 \times 10^{-2}\ \text{Å}^{-1} \quad \text{for } D_{11}$$

$$10^{-2} < q < 2 \times 10^{-1}\ \text{Å}^{-1} \quad \text{for } D_{17}$$

The neutron wavelength is $\lambda = 10$ Å in both cases and the cadmium sample holder has a circular hole diameter of 10 mm. The elliptic disc shape samples with a roughly 14 mm long axis and 10 mm small axis cover the entire diaphragm area.

The scattered intensities for all orientations of the scattering vector in the plane of the band are recorded on a bidimensional detector consisting of 64×64 cells[11].

The incoherent contribution to the total intensity is evaluated from the scattering of a purely protonated identical sample scaled to the precise concentrations of hydrogenated and deuterated chains in the mixture. Apart from incoherent background subtractions, transmission corrections and normalization to the totally incoherent scattering of water are also undertaken. The resulting coherent scattering spectra are then analysed using anisotropic data treatment available at ILL in order to obtain the scattered intensities along $\hat{x}_1$ ($I(q_\parallel)$) and $\hat{x}_2(I(q_\perp))$[12].

The coherent differential scattering cross-section is expressed as:

$$I(q) = (b_D - b_H)^2 \times dN/M \times \phi_D(I - \phi_D)g(q)$$

where b_D and b_H are the scattering lengths of the deuterated and hydrogenated monomers respectively, d is the density, N, is the Avogadro number and M the molar mass (dN/M is thus the total number of monomers per unit volume), ϕ_D is the volume fraction of deuterated monomers and $g(q)$ is the single chain scattering function.

For gaussian coils in the bulk $g(q) = g_D(q)$ is the Debye scattering function which has been modified to introduce polydispersity effects:

$$g_D(q) = \frac{2}{(U+1)\xi^2}[(1+U\xi)^{-(1/U)} - 1 + \xi] \qquad (1)$$

where $\xi = \langle R^2 \rangle q^2/(1+2U)$ and $U = M_w/M_n - 1$ is a measure of polydispersity. $\langle R^2 \rangle$ is the mean square radius of gyration which is a z-average in the case of SANS, i.e. $\langle R^2 \rangle = \langle R^2 \rangle_z$. Correction to the weight average may be effected by introducing the polydispersity effects in the form[14]

$$\langle R^2 \rangle_w = \langle R^2 \rangle_z \frac{1+U}{1+2U} \qquad (2)$$

A further correction is also required to account for the mismatch between deuterated and hydrogenated molecular weight distributions. In fact this correction proves to be negligible at low deuterated polymer concentrations.

In analysing the data we shall consider successively two domains of momentum transfer:

(i) The Guinier range defined as: $q < R_g^{-1}$ where R_g is the radius of gyration of the chain.

The intensity is expressed as

$$I(q) \sim 1 - \frac{q^2 \langle R^2 \rangle_z}{3}$$

from which the mean square radius of gyration may be extracted in the classical Zimm representation $I^{-1}(q) = f(q^2)$. Note that due to slight polydispersity

Table 1 Summary of experimental conditions

	ϕ_D[a]	M_w^{Db}	M_w/M_n^{Db}	M_w^{Hb}	M_w/M_n^{Hb}	T_{def}[c] (K)	$\dot{\varepsilon}_p$ (s^{-1})	Mode[d]
PS I	0.10	100 000	1.17	223 000	1.17	290	5.10^{-4}	gl.[e]
						307	5.10^{-6}	dif.
PS II	0.06	243 000	1.45	223 000	1.17	242	5.10^{-4}	gl.
						290	5.10^{-4}	gl.
PS III	0.10	1 280 000	1.15	952 000	1.19	287	$4.5.10^{-6}$	dif.
							$1.8.10^{-3}$	gl.
PMMA	0.03	184 000	1.35	148 000	1.84	256	4.10^{-4}	dif.
						290	4.10^{-4}	dif.

[a] ϕ_D is the weight fraction of deuterated species
[b] Superscripts D and H refer to deuterated and hydrogenated polymers respectively
[c] T_{def} is the deformation temperature
[d] gl. refers to the glide mode and dif. to the diffusional mode
[e] This experiment was mistakenly quoted with $T_{def} = 250$ K in our previous paper (*Table 2* 'Glide' set 2). This error did not alter our conclusions

effects determination of $\langle R^2 \rangle_z$ is still accurate for $q \times R_g \sim 1$. Furthermore determination of $\langle R^2 \rangle_z$ (either in the isotropic R_0 situation or in the deformed state, i.e. $R_\parallel$ and $R_\perp$) does not require any specific assumption on the intramolecular form factor.

(ii) The intermediate range defined as: $R_g^{-1} < q < b^{-1}$ where b is the statistical length of the chain. As long as there is no deviation to the Debye scattering law, $I(q)$ should be proportional to q^{-2}.

$$I(q) \sim \frac{2}{q^2 \langle R^2 \rangle_z}$$

Regarding the simple shear situation, we previously recalled that:

$$R_\perp = R_0 \text{ (along } \hat{x}_2)$$

and

$$R_\parallel = \lambda R_0 \text{ (along } \hat{x}_1)$$

where $\lambda^2 = 1 + tg^2\gamma$.

Under the assumption of affine deformation over the entire range of correlation distances one would thus expect:

$$I_\perp \sim \frac{2}{q^2 R_\perp^2} \sim I_{iso}$$

and

$$I_\parallel \sim \frac{2}{q^2 R_\parallel^2} = \frac{2}{q^2 \lambda^2 R_0^2} \sim \frac{1}{\lambda^2} I_{iso}$$

This case will be more conveniently considered in the Kratky representation of the scattered intensity, $q^2 I \times I(q) = f(q)$.

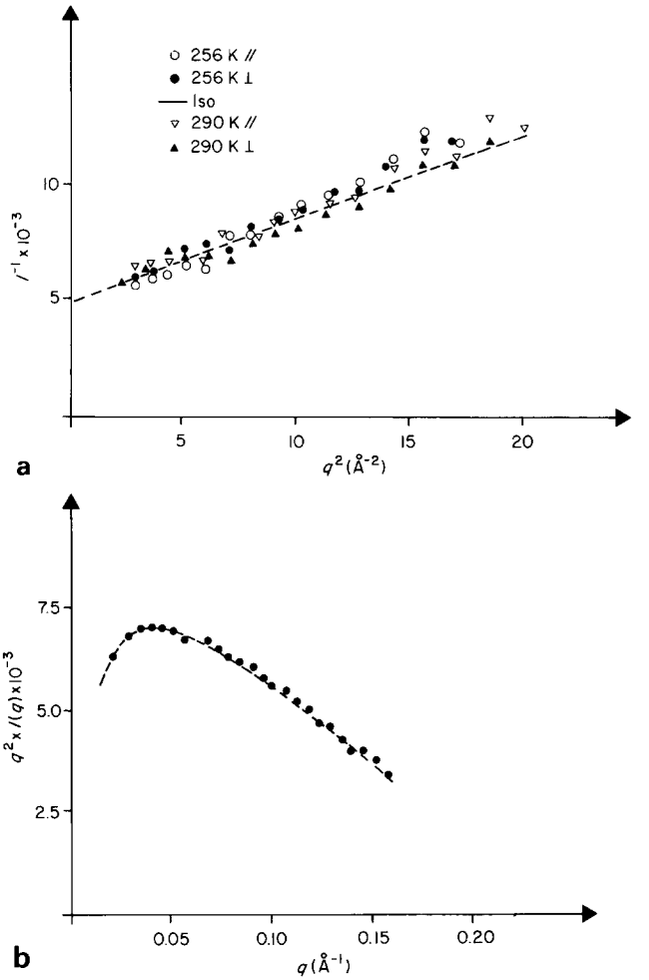

Figure 3 (a) Zimm representation of the scattering intensity in the Guinier range for PMMA. (b) Kratky plot for isotropic PMMA in the intermediate q range

RESULTS

The case of PMMA

A Zimm plot in the Guinier range is shown in *Figure 3a* which compares the behaviour of an isotropic sample with the ones of two samples deformed in the diffusional mode. Apart from a scatter of the data around the isotropic curve no marked anisotropy can be noticed.

Recently Dettenmaier *et al.*[15] reported on a SANS characterization of PMMA samples stretched to a draw ratio of 2.2 at temperatures between $0.85 \times T_g$ and T_g. They found that deformation is essentially affine from the macroscopic strain tensor down to the molecular level. This situation is not contradictory and further comments will be given in the discussion.

Table 2 summarizes our results in terms of $\langle R^2 \rangle_z^{1/2}$. Converting the isotropic radius of gyration to its weight average value yields $\langle R_0^2 \rangle_w^{1/2} = 132 \pm 10$ Å which is 12% higher than the value calculated from the $\langle R^2 \rangle_w = f(M_w)$ relationship given by Kirste *et al.*[16]. Such a discrepancy might be due to a different tacticity of our polymer.

Finally, in the isotropic (undeformed case), a Kratky plot in the intermediate range (*Figure 3b*) exhibits a strong departure from the gaussian plateau, the drop in $q^2 \times I(q)$ beyond q values of the order of 0.05 Å^{-1} is consistent with previous work and has been shown to reflect specific local chain configurations in PMMA[16,17].

Table 2 Experimental results – PMMA – Guinier range

$R_0 = \langle R_{iso}^2 \rangle_z^{1/2}$ (Å)	T_{def} (K)	$R_\perp$ (Å)	R (Å)	Mode
150	256	160	160	dif.
150	290	155	155	dif.

The case of PS

Since macroscopic shear bands could be developed more successfully over the entire range of temperatures and strain-rates, this polymer has been studied more extensively. We shall consider successively the glide and diffusional mode.

A summary of the measured radii of gyration deduced from the scattering in the Guinier range is given in *Table 3* and illustrated for PS II in *Figure 4a* which compares the behaviour of the PS samples deformed in the glide mode to the one of undeformed PS. The data could not be considered at q values below 7×10^{-3} Å^{-1} because of a sharp increase in the intensity presumably due to the diffusion of microvoids. In fact fitting experimental data to equation (1) has shown that for this fairly polydisperse material, the radii of gyration could be determined from a Zimm plot in a q range slightly above the Guinier range, i.e. for $1 < q \times R < 2.5$[2a].

Table 3 Experimental results – PS – Guinier range

	$R_0=\langle R^2_{iso}\rangle_z^{1/2}$ (Å)	$T_{def.}$ (K)	Mode	$R_{\perp}$ (Å)	$R_{\parallel}$ (Å)	λ	$tg\gamma$	γ
PS I	95	290	gl.	96	117	1.22	0.7	35
PS II	165	242	gl.	172	252	1.48	1.09	47
PS II	165	290	gl.	170	200	1.19	0.65	33
PS I	95	307	dif.	96	96			

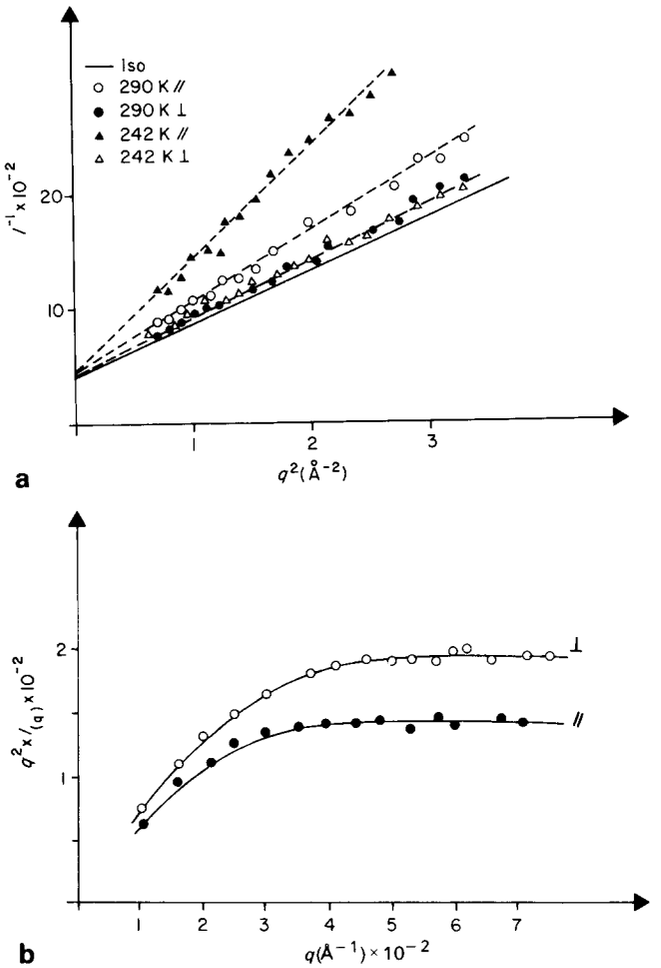

Figure 4 (a) Zimm representation of the scattering intensity in the Guinier range for PS II. (b) Kratky plot in the intermediate q range for PS I in the glide mode

In all situations weight average radii of gyration deduced from equation (2) agree within experimental error ($\Delta R/R<10\%$) to the relation given by Cotton *et al.*[18] $\langle R^2_{iso}\rangle_w^{1/2}=0.28\,M_w^{1/2}$ Å.

In the case of PS III with a large molecular weight the radius of gyration could not be deduced from the scattering curves. We may already notice regarding this glide mode that the dimension along $\hat{x}_2$, i.e. $R_{\perp}$ is almost unaffected as compared to R_0, in excellent agreement with our assumptions of simple shear and with our macroscopic observations of the transverse dimension of the samples.

On the other hand, we can remark, in the case of PS II, that as it was expected the coil anisotropy increases with decreasing temperature.

As can be seen in *Figure 4b*, in the intermediate q range, the Kratky plot for PS I shows the characteristic Debye plateau in both parallel and transverse directions. With the assumption of affine deformation over the entire q range the ratio of plateau heights $q^2I_{\parallel}/q^2I_{\perp}$ should be equal to λ^{-2}, leading to a value $\lambda=1.19$ which is in good agreement with the one found in the Guinier range (*Table 3*): $\lambda=1.22$.

In *Figure 5*, isointensity contours plots (in arbitrary units) for PS III in the intermediate range compare the behaviour of the glide mode (*Figure 5a*) to that of the diffusional mode (*Figure 5b*) (refer to *Table 1* for experimental conditions). The main axis of the elliptic shear band lies along the diagonals of the square. A more complete investigation of the anisotropic situation in the intermediate and large q range using different polymer labellings will be given elsewhere for this particular set of experiments.

Returning to the diffusional mode, radii of gyration data (line 4 of *Table 3*) confirm previously published data where no coil anisotropy could be detected[7]. To account for the imposed deformation a tentative explanation in terms of coil intercalation was proposed, which implies a motion of the centre of gravity of the coils through cooperative displacements along the chains[2a] akin to reptation motions. In fact if such cooperative motions are expected to keep the overall chain configuration unchanged for a polymer coil of 1000 monomer units ($M\sim100\,000$), then for the same deformation time allowed (i.e. for the same strain and strain-rate) the distribution of chain segments in a much larger molecule (say 10 000 units) should be noticeably altered.

The actual scattering behaviour for PS III ($M_w=1\,280\,000$) in the diffusional mode as seen in *Figures 5b* and *6* does not differ from the low molecular weight pattern (see Figures 2 and 4 in ref. 7). It exhibits the same small departure from the isotropic curve and one hardly notices a slight distinction between the longitudinal and transverse intensities, the interpretation of the experimental findings in the diffusional mode has to be found elsewhere; this will be the object of the final discussion.

DISCUSSION

We recalled above that the shear angle could be deduced from the measured longitudinal and transverse radii through the equation:

$$R_{\parallel}/R_{\perp}=\lambda=\sqrt{1+tg^2\gamma}$$

The last three columns of *Table 3* give a summary of the values deduced in the glide mode. It clearly disagrees with the range of shear strains reported from macroscopic observations on the split samples ($1.15<tg\gamma<1.30$). This certainly does not mean that deformation is non-affine since the SANS experiments bring forth evidence for affine deformation over the entire q-range and there is no

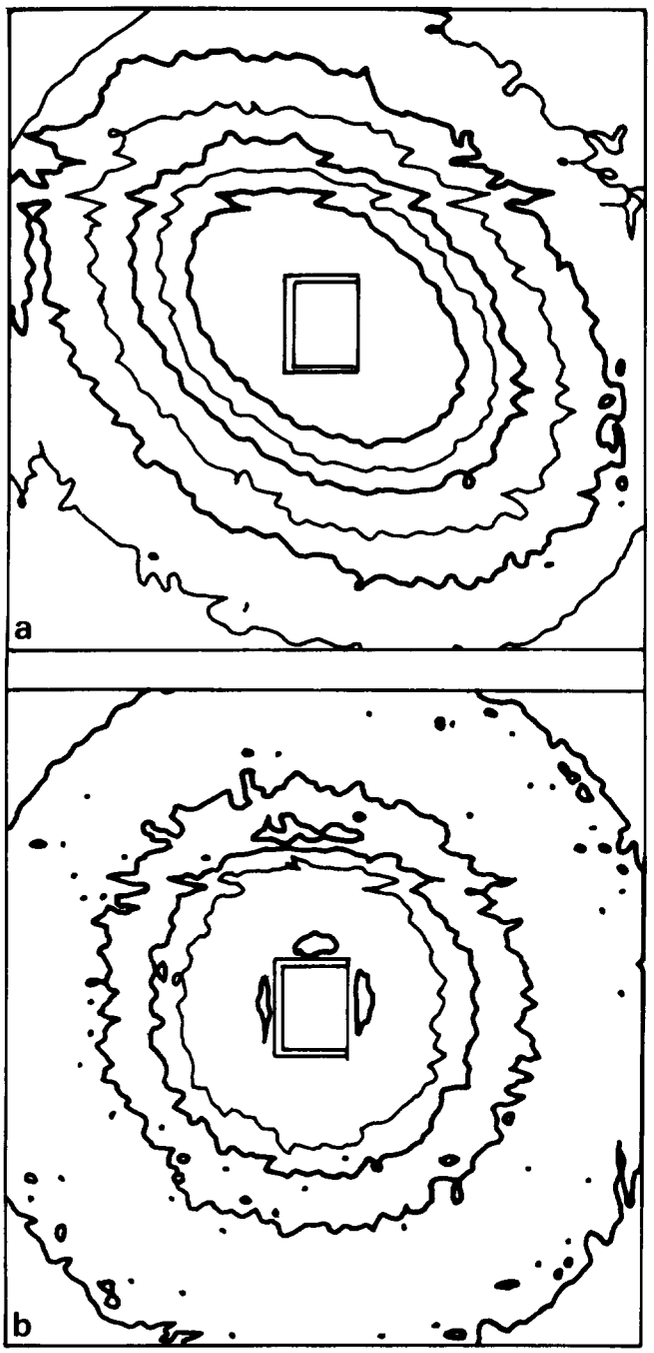

Figure 5 Isointensity contour plots for PS III in the glide (a) and diffusional (b) modes

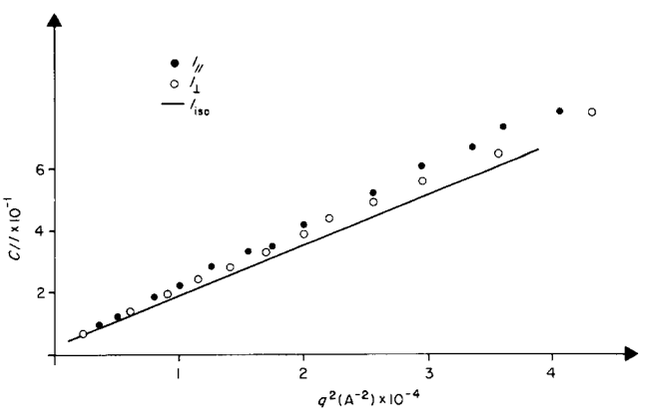

Figure 6 Zimm representation of the scattering intensity in the intermediate range for PS III in the diffusional mode

structural reason why affinity should break from the millimetre scale down to the 10^3 Å scale.

In fact considering the shear bands produced in our compression tests, it appears that even if deformation is fairly homogeneous in the middle of the band, lateral external surface effects perturb a non negligible fraction of the volume submitted to SANS. Thus any anisotropy deduced from the average form factor of the coils will be underestimated, or else speaking the true comparison should be made with a precise two dimensional macroscopic strain characterization of the band. In addition we notice that the lower the temperature (242 K) for a comparable strain-rate, the better the confinement to a narrow band that is obtained, in agreement with the situation of being far enough below the temperature T_c which depicts the gradual transition from pure glide to the molecular relaxation aided diffusional mode.

If we now consider the diffusional mode, a 20 to 30% underestimation of the anisotropy as seen in the SANS experiment would mean a ratio $\lambda < 1.1$.

Moreover our diffusional mode relates to the predominantly diffuse zone regime quoted in the literature[9,10]. Such diffuse zones have been reported to consist of extremely fine bands not as localized and continuous as the coarse slip bands of the glide mode[10]. This means that the microscopic slip systems do not necessarily lie parallel to our macroscopic band, which would be an additional factor in reducing the apparent anisotropy in the SANS experiments and thus having a ratio $R_{\parallel}/R_{\perp} < 1.10$ falls within experimental error and is consistent with our observations.

To sum up, this attempt to characterize molecular deformation at yield for temperatures well below T_g using SANS encounters some limitations, due to the fact that yielding is a process essentially heterogeneous in nature with the additional drawback that a compression tested sample cannot be directly investigated by any scattering technique. Nevertheless as long as the microscopic glide systems retain the same geometric parameters as the macroscopic shear band, molecular anisotropy can be depicted over the entire q range. In such a case the non-ability to relate precisely macroscopic strains to the coils strains does not imply a non-affine behaviour at that particular scale.

In the same way the failure to get information from the SANS in the diffusional mode is indeed inherent to a change in the elementary slip mechanisms as evidenced by the thermodynamic analysis of plasticity. In that regime one has to reach a homogeneously drawn situation with extension ratios above 2 as reported by Dettenmaier *et al.*[15] to be able to prove a noticeable coil shear strain.

We would conclude by saying that the same simple shear geometry has to be considered from the sample scale down to the molecular level; the molecular layers are sheared past each other by the same amount in the 100–200 Å range as well as down to the 20 Å range. This features nothing else than a dislocation nature of the shear defects responsible for yielding deformation[19].

This view might bring some light on the origin of a much smaller coil anisotropy found in samples deformed above T_c: this fact might come simply from a wider spacing between elemental slip lines at higher temperatures, due to some local relaxation available in the polymer, in contrast to adjacent slip lines at lower temperatures.

ACKNOWLEDGEMENTS

We would like to thank P. Marie and M. Rawiso for their help during the course of the experiments performed at the Institut Laüe-Langevin, Grenoble.

REFERENCES

1 Escaig, B. and Lefebvre, J. M. *Rev. Phys. Appliquée* 1978, **13**, 285
2 (a) Lefebvre, J. M. *Thèse de doctorat*, University of Lille, 1982; (b) Escaig, B. 'Plastic deformation of Amorphous and semi-crystalline Materials' (Eds. B. Escaig and C. G'sell), Les Editions de Physique, Les Ulis, France, 1982, p. 187
3 Cavrot, J. P., Haussy, J., Lefebvre, J. M. and Escaig, B. *Mater. Sci. Eng.* 1978, **36**, 95
4 Haussy, J., Cavrot, J. P., Escaig, B. and Lefebvre, J. M. *J. Polym. Sci. Polym. Phys. Edn.* 1980, **18**, 311
5 Lefebvre, J. M. and Escaig, B. *J. Mater. Sci.* 1985, **20**, 438
6 Lefebvre, J. M. and Escaig, B., to be published
7 Lefebvre, J. M., Escaig, B. and Picot, C. *Polymer* 1982, **23**, 1751
8 Argon, A. S., Andrews, R. J., Godrick, J. A. and Whitney, W. *J. Appl. Phys.* 1968, **39**, 1899
9 Bowden, P. B. and Raha, S. *Phil. Mag.* 1970, **22**, 463
10 Wu, J. B. C. and Li, J. C. M. *J. Mater. Sci.* 1976, **11**, 434
11 Ibel, K. *J. Appl. Crystallogr.* 1978, **9**, 296
12 Ghosh, R. 'A computing guide for SANS experiments', ILL, Grenoble, 1981
13 Greschner, G. S. *Makromol. Chem.* 1970, **170**, 203
14 Altgelt, K. and Schultz, G. V. *Makromol. Chem.* 1960, **36**, 209
15 Dettenmaier, M., Higgins, J. S., Kausch, H. H., Maconnachie, A. and Nguyen, T. Q. Europhysics Conf., Hamburg, 1983, to be published
16 Kirste, R. G., Kruse, W. A. and Ibel, K. *Polymer* 1975, **16**, 120
17 Yoon, D. Y. and Flory, P. J. *Macromolecules* 1976, **9**, 299
18 Cotton, J. P., Decker, D. and Benoit, H. *et al.*, *Macromolecules* 1974, **7**, 863
19 Escaig, B. *Polym. Eng. Sci.* 1984, **24**, 737